SNAT7 is the primary lysosomal glutamine exporter required for extracellular protein-dependent growth of cancer cells

Verdon, Quentin; Boonen, Marielle; Ribes, Christopher; Jadot, Michel; GASNIER, Bruno; Sagné, Corinne

Published in:
Proceedings of the National Academy of Sciences of the United States of America

DOI:
10.1073/pnas.1617066114

Publication date:
2017

Document Version
Publisher's PDF, also known as Version of record

SNAT7 is the primary lysosomal glutamine exporter required for extracellular protein-dependent growth of cancer cells

Quentin Verdon[a], Marielle Boonen[b], Christopher Ribes[a], Michel Jadot[b], Bruno Gasnier[a,1], and Corinne Sagné[a,1]

[a]Neurophotonics Laboratory, Paris Descartes University, CNRS UMR 8250, Sorbonne Paris Cité, F-75006 Paris, France; and [b]Unité de Recherche en Physiologie Moléculaire (URPhyM), Laboratoire de Chimie Physiologique, Narilis, University of Namur, 5000 Namur, Belgium

Edited by Robert H. Edwards, University of California, San Francisco, CA, and accepted by Editorial Board Member Pietro De Camilli March 27, 2017 (received for review November 9, 2016)

Lysosomes degrade cellular components sequestered by autophagy or extracellular material internalized by endocytosis and phagocytosis. The macromolecule building blocks released by lysosomal hydrolysis are then exported to the cytosol by lysosomal transporters, which remain undercharacterized. In this study, we designed an in situ assay of lysosomal amino acid export based on the transcription factor EB (TFEB), a master regulator of lysosomal biogenesis that detects lysosomal storage. This assay was used to screen candidate lysosomal transporters, leading to the identification of sodium-coupled neutral amino acid transporter 7 (SNAT7), encoded by the SLC38A7 gene, as a lysosomal transporter highly selective for glutamine and asparagine. Cell fractionation confirmed the lysosomal localization of SNAT7, and flux measurements confirmed its substrate selectivity and showed a strong activation by the lysosomal pH gradient. Interestingly, gene silencing or editing experiments revealed that SNAT7 is the primary permeation pathway for glutamine across the lysosomal membrane and it is required for growth of cancer cells in a low free-glutamine environment, when macropinocytosis and lysosomal degradation of extracellular proteins are used as an alternative source of amino acids. SNAT7 may, thus, represent a novel target for glutamine-related anticancer therapies.

lysosome | transporter | glutamine | cell nutrition | cancer

Lysosomes are single-membrane organelles acting as major recycling sites in eukaryotic cells. They are equipped with acidic hydrolases and degrade aged or damaged macromolecules and organelles sequestered or internalized by the autophagy, endocytosis, and phagocytosis pathways. The macromolecule building blocks (amino acids, sugars, nucleosides, etc.) released by these hydrolases are then exported to the cytosol by lysosomal transporters for reuse in cellular metabolism. In addition to this well-known catabolic role, lysosomes have been involved in other cellular functions, such as lysosomal cell death (1), cell membrane repair (2), and cell homeostasis, in which they act as signaling hubs for activation of the mechanistic target of rapamycin complex 1 (mTORC1), a master regulator of growth and metabolism (3). Lysosomes also participate in a transcriptional feedback loop that adapts lysosomal degradation to cellular needs (4).

Finally, lysosomes, especially lysosomal transporters, also play a role in cell nutrition by providing an alternative route to nutrients and micronutrients that do not readily cross the plasma membrane. For instance, cellular uptake of cobalamin, which tightly binds transcobalamin II in extracellular fluids, involves receptor-mediated endocytosis of the transcobalamin/cobalamin complex, degradation of transcobalamin in the lysosomal lumen, and lysosomal export of free cobalamin through a process requiring the membrane proteins ABCD4 and LMBD1 (5–7). Nutrients may also be internalized without membrane receptors by fluid-phase endocytosis (pinocytosis) or macropinocytosis. For instance, external free sialic acids enter cells through pinocytosis and lysosomal export by the sialic acid transporter sialin (8, 9). This two-step indirect route accounts for the metabolic incorporation of the dietary, nonhuman sialic acid *N*-glycolylneuraminic acid into human cell glycans (10). Recently, lysosomes have been similarly shown to participate in an "opportunistic" nutrition route of cancer cells when free amino acids are scarce in their environment (11). Under such conditions, lysosomal degradation of internalized extracellular proteins and lysosomal amino acid export can compensate for the lack of free amino acid uptake at the plasma membrane. For instance, Ras-activated cancer cells acquire glutamine, an amino acid essential to their proliferation, through macropinocytosis of extracellular proteins (12).

In this study, we investigated the molecular and cellular functions of a poorly characterized member of the solute carrier 38 (SLC38) family, also known as the sodium-coupled neutral amino acid transporter (SNAT) family. This family includes 11 members in the human genome, which, for the best characterized, are divided in two subgroups: system A and system N transporters. System A transporters (SNAT1, SNAT2, and SNAT4) have a broad selectivity for neutral amino acids, which they cotransport with one Na^+. System N transporters (SNAT3, SNAT5, and possibly SNAT8) prefer glutamine, asparagine, and histidine over small neutral amino acids, and their ion-coupling mechanism is more complex, with an antiport of proton in addition to the cotransport of Na^+ and the coexistence of multiple transport modes (13, 14).

SNAT9, also known as SLC38A9, stands out in this family because it was recently characterized as a slow, broadly selective amino acid transporter involved in amino acid-sensing and

Significance

Lysosomes are degradative intracellular organelles essential to cell maintenance and homeostasis. Although their degradative function is well documented, the proteins responsible for the efflux, and reuse, of lysosomal degradation products remain largely unknown. In this study, we identify the transporter responsible for lysosomal efflux of glutamine, an amino acid central to several key metabolic pathways. This central role of glutamine is exploited by several types of cancer cells with increased consumption of glutamine. Interestingly, genetic inactivation of the transporter impairs their growth under conditions of limited glutamine availability when internalized extracellular proteins are used as an alternative source of amino acids, suggesting novel approaches for anticancer therapies.

Author contributions: B.G. and C.S. designed research; Q.V., M.B., C.R., and C.S. performed research; Q.V., M.B., M.J., B.G., and C.S. analyzed data; and Q.V., B.G., and C.S. wrote the paper.

Conflict of interest statement: The authors have filed a European patent application on potential therapeutic uses of SNAT7-directed tools.

This article is a PNAS Direct Submission. R.H.E. is a guest editor invited by the Editorial Board.

[1]To whom correspondence may be addressed. Email: bruno.gasnier@parisdescartes.fr or corinne.sagne@parisdescartes.fr.

This article contains supporting information online at www.pnas.org/lookup/suppl/doi:10.1073/pnas.1617066114/-/DCSupplemental.

signaling to mTORC1 at the lysosomal membrane (15, 16). In particular, SNAT9 interacts with the Ragulator/Rag GTPase complex in an amino acid-dependent manner, and mTORC1 fails to be activated by amino acids, especially arginine, in its absence. It was thus suggested that SNAT9 acts as a transceptor, that is, a transporter-like protein with receptor function (17), rather than as a genuine amino acid transporter (15, 16, 18).

In a recent study of the lysosomal proteome, we unambiguously detected SNAT7 in the lysosomal membrane (19). SNAT9 was also detected in a lysosome-specific manner in that study, yet only in a single biological replicate of three, preventing its inclusion in our proteome list. Expression of a recombinant SNAT7 fused to GFP colocalized with LAMP1, a marker of late endosomes and lysosomes, thus corroborating our proteomic finding (19). In this study, we establish the lysosomal localization of the native protein and show that SNAT7 transports glutamine and asparagine, but not other amino acids, in an acidic pH-stimulated manner, and that it represents the primary permeation pathway for these amino acids across the lysosomal membrane. Moreover, we show that SNAT7 is required for nutrition of cancer cells in a low free-glutamine environment, when macropinocytosis and lysosomal degradation of extracellular proteins are used as an alternative source of amino acids to sustain cell growth.

Results

A TFEB-Based Live-Cell Assay of Lysosomal Amino Acid Transporters. To screen for potential lysosomal amino acid transporters, we developed an assay based on the indirect detection of lysosomal stress induced by amino acid overload in live cells. Lysosomal stress can be monitored using the master transcription factor EB (TFEB), which regulates lysosomal biogenesis and autophagy, and adapts them to degradative needs of eukaryotic cells (20). Under unstressed, nutrient-replete conditions, TFEB is phosphorylated by mTORC1 at the lysosomal surface, resulting in its cytosolic retention and inhibition (21–23). However, when macromolecules or small molecules accumulate in lysosomes, TFEB is dephosphorylated and translocated to the nucleus, where it activates lysosomal and autophagy genes (4, 20). We, thus, reasoned that artificial overload of lysosomes with a specific amino acid in live cells should induce nuclear translocation of TFEB. Because most lysosomal metabolite transporters export their substrates to the cytosol, overexpression of a cognate transporter for the tested amino acid should reduce lysosomal overload and, consequently, reduce nuclear translocation of TFEB (Fig. 1*A*).

To overload lysosomes artificially with amino acids, we used an old biochemical trick that consists of the application of amino acid esters. Esters readily permeate biological membranes, and ester hydrolysis in the acidic, hydrolase-rich lysosome generates a free amino acid build-up within its lumen (24). This approach has traditionally been used with subcellular fractions. However, we recently observed that it can significantly load lysosomes with amino acids in live cells as well (figure 6F of ref. 25), indicating that a significant proportion of uncleaved ester reaches lysosomes despite the presence of cytosolic esterases.

We, thus, applied diverse amino acid esters to HeLa cells transiently expressing a monomeric red fluorescent protein (mRFP)/TFEB fusion protein and tested whether they induce lysosomal stress. The mRFP-TFEB intracellular distribution was classified in three categories, nuclear, cytosolic, and mixed, to provide a semiquantitative measurement of lysosomal stress (Fig. 1*B*). Several amino acid esters activated mRFP-TFEB in a dose-dependent manner (representative examples are shown in Fig. S1). A concentration-inducing nuclear translocation of mRFP-TFEB (nuclear + mixed distributions) in about 40% of cells was selected for each ester to detect whether additional treatments alter lysosomal overload with a good sensitivity. For glutamine, we used an ester made with an alcohol group (tert-butanol) more hydrophobic than methanol to reach this level of lysosomal stress (Fig. S1).

Next, we coexpressed known lysosomal transporters with mRFP-TFEB and tested whether they protect cells from the artificial amino acid overload. Plasmid transfection induced transient nuclear translocation of mRFP-TFEB (which vanished after 48 h), highlighting the sensitivity of the mTORC1/TFEB pathway to diverse internal cues. We used a well-targeted, inactive lysosomal sugar transporter [human sialin P334R (9)] as a negative control to address the possibility that lysosomal membrane protein overexpression might also induce lysosomal stress independent of any luminal overload. Interestingly, these experiments showed that overexpression of the lysosomal amino acid exporters LYAAT1 (26) and PQLC2 (25) selectively reduced the lysosomal stress caused by esters of their cognate amino acids (alanine and lysine, respectively), but not by esters of nontranslocated amino acids (Fig. 1*B*). In contrast, the inactive lysosomal sugar transporter had no effect in any tested condition (Fig. 1*B*). Our TFEB-based live-cell assay, thus, successfully detects the build-up of amino acids in lysosomes and, conversely, their depletion by lysosomal transporters.

We used this assay to screen orphan lysosomal membrane proteins or poorly characterized lysosomal transporters for amino acid transport. In a recent proteomic study, we identified several protein candidates, including SNAT7, a poorly characterized member of the SLC38 transporter family (19). A set of 11 tractable amino acid esters was screened against SNAT7 in our assay to identify its putative substrates. HeLa cells expressing PQLC2 provided a positive control (lysine methyl ester) and negative controls (other esters) in these experiments. Fig. 1*C* shows the mean outcome of three independent experiments. As expected, PQLC2 reduced the lysosomal overload of lysine, but not of neutral and anionic amino acids, in agreement with the cationic amino acid selectivity of its transport function (25, 27). In contrast, SNAT7 overexpression selectively decreased the lysosomal stress induced by asparagine and glutamine esters, but not by other amino acid esters (Fig. 1*C*). We concluded that SNAT7 selectively exports asparagine and glutamine from the lysosome.

Subcellular Localization of Native SNAT7 in HeLa Cells. In our previous study, we validated the selective proteomic detection in lysosome-enriched fractions by showing that a recombinant construct (EGFP-SNAT7) colocalizes with late endosomes and lysosomes in HeLa cells (19). To get additional evidence for the native protein, we examined its intracellular distribution by subcellular fractionation. Human SNAT7 (hSNAT7) was detected on immunoblots using a polyclonal antibody directed against the 53 first amino acids (HPA041777; Atlas Antibodies). In HeLa cell homogenates, HPA041777 immunoreactivity was mostly associated with a 40-kDa band (Fig. 2*B*). To confirm the identity of this band, we inactivated the *SLC38A7* gene, which encodes SNAT7, in HeLa cells using the CRISPR/Cas9 nickase method for genome editing (28). In agreement with our HeLa clone genomic sequences, homozygous disruption of *SLC38A7* selectively abolished the 40-kDa band, showing that it corresponds to native SNAT7 (Fig. 2 *A* and *B*).

We next analyzed the behavior of the SNAT7 band on subcellular fractionation, because the antibody could not be used to detect endogenous levels of the protein by immunofluorescence (Fig. S2). HeLa cells were first subjected to a classical differential centrifugation method (29). In this protocol (Fig. 2*C*), SNAT7 was strongly enriched in the L fraction (enriched in lysosomes) with only minor signal in the M fraction (which contains the bulk of mitochondria) and the P fraction (in which most of the peroxisome and microsome populations are recovered). Moreover, the quantitative distribution profile of SNAT7 was very similar to the profile of the lysosomal marker, and clearly distinct from the profiles of other cell compartments, including the plasma membrane (Fig. 2*D* and Fig. S3). Fractions M and L were then pooled

and further fractionated using isopycnic centrifugation on a linear sucrose density gradient. This technique showed that SNAT7 perfectly codistributes with the lysosomal marker, but not with mitochondrial, endoplasmic reticulum, and peroxisomal markers (Fig. 2*D* and Fig. S3). Plasma membrane vesicles overlapped with lysosomes in this gradient. However, most of them were discarded from the pooled M + L fractions, and the contrasting profiles of SNAT7 and the plasma membrane marker in the differential centrifugation protocol indicate that the plasma membrane pool of SNAT7, if any, is, at most, a minor part of the total pool. We concluded that native SNAT7 is a resident lysosomal protein.

SNAT7 Is the Primary Permeation Pathway for Glutamine and Asparagine Across the Lysosomal Membrane. An earlier study reported that SNAT7 is a promiscuous plasma membrane transporter that recognizes a high diversity of amino acids, including alanine, arginine, and glutamine at least (30). However, we could not replicate these data, and we could not measure reliable uptake signals when SNAT7-expressing *Xenopus* oocytes were incubated in an acidic medium to mimic the environment faced by SNAT7 in the lysosomal membrane. Artificial redirection to the cell surface by mutation of lysosomal sorting motifs has established robust transport assays for several lysosomal transporters (9, 25, 31).

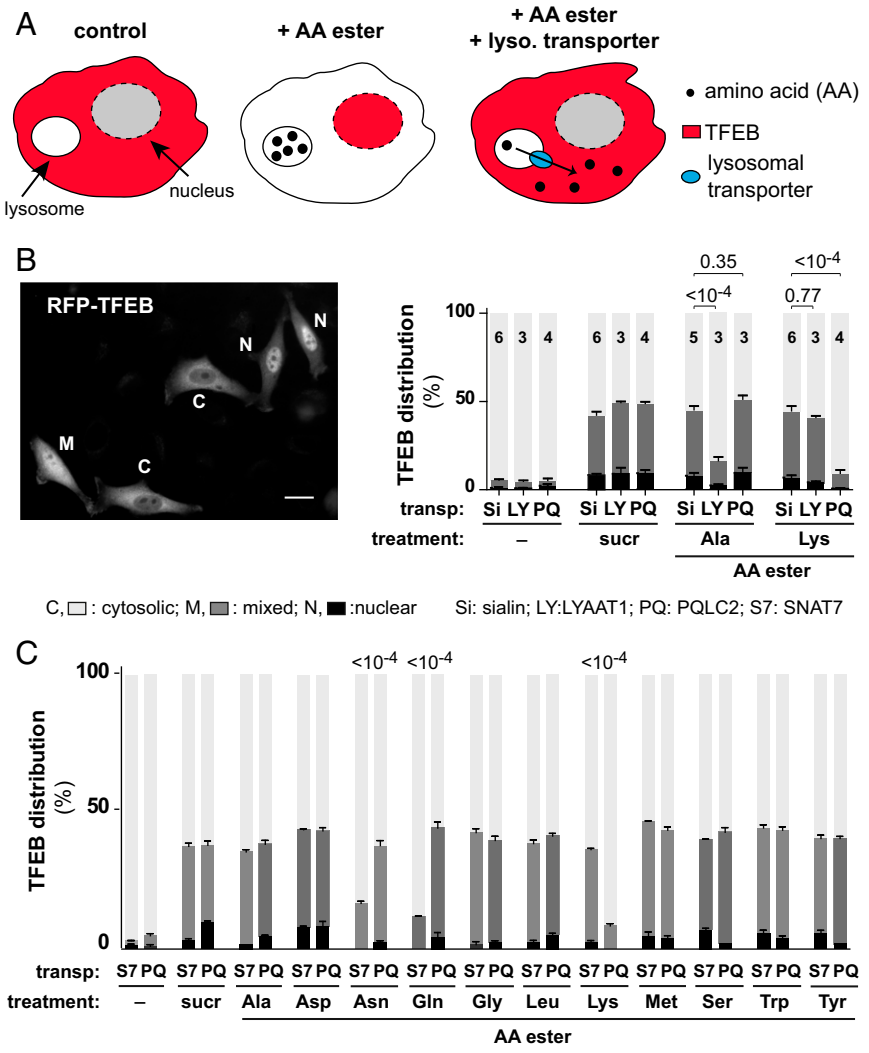

Fig. 1. Live-cell assay reveals that SNAT7 selectively exports asparagine and glutamine from lysosomes. (*A*) Principle of the TFEB-based assay. (*Left*) In untreated HeLa cells, the transcription factor TFEB mainly localizes to the cytosol. (*Center*) Treating cells with an amino acid (AA) ester results in intralysosomal overload of the corresponding amino acid, which in turn induces TFEB translocation to the nucleus. (*Right*) Overexpression of a lysosomal transporter that exports the amino acid out of lysosomes reduces lysosomal stress and, consequently, TFEB nuclear translocation. (*B*) Proof-of-concept experiment. HeLa cells were transiently cotransfected with plasmids encoding mRFP-TFEB and one of the three well-characterized lysosomal transporters fused to EGFP, sialin (Si), LYAAT1 (LY), and PQLC2 (PQ), which export sialic acid, alanine, and lysine, respectively, from lysosomes. In the case of sialin, we used a nontransporting mutant (P334R) to serve as a negative control. Two days after transfection, cells were treated with 100 mM sucrose or with the indicated amino acid esters at an optimal concentration (*Results* and *Materials and Methods*) for 2 h before fixation. The mRFP-TFEB intracellular localization (cytosolic, nuclear, or mixed) was determined under a fluorescence microscope, as shown in the photograph, for at least 50 EGFP-positive cells per condition. (Scale bar: 10 μm.) The graph shows the mean outcome of the number of experiments indicated on the bars. Treating cells with sucrose or amino acid esters induces nuclear translocation of TFEB in ∼50% of cells. However, TFEB translocation was reduced to 25% and 10%, respectively, in LYAAT1- and PQLC2-expressing cells treated with an ester of a translocated amino acid (alanine and lysine, respectively). (*C*) HeLa cells transiently expressing mRFP-TFEB and either rPQLC2-EGFP (PQ) or EGFP-mSNAT7 (S7) were treated with sucrose or one of the indicated amino acid esters for 2 h before fixation, and the TFEB localization measurement was performed as in *B*. The graph displays the mean outcome of three independent experiments. SNAT7 overexpression selectively decreases the lysosomal stress induced by asparagine and glutamine overload. Error bars represent SD. *P* values are shown above the bars.

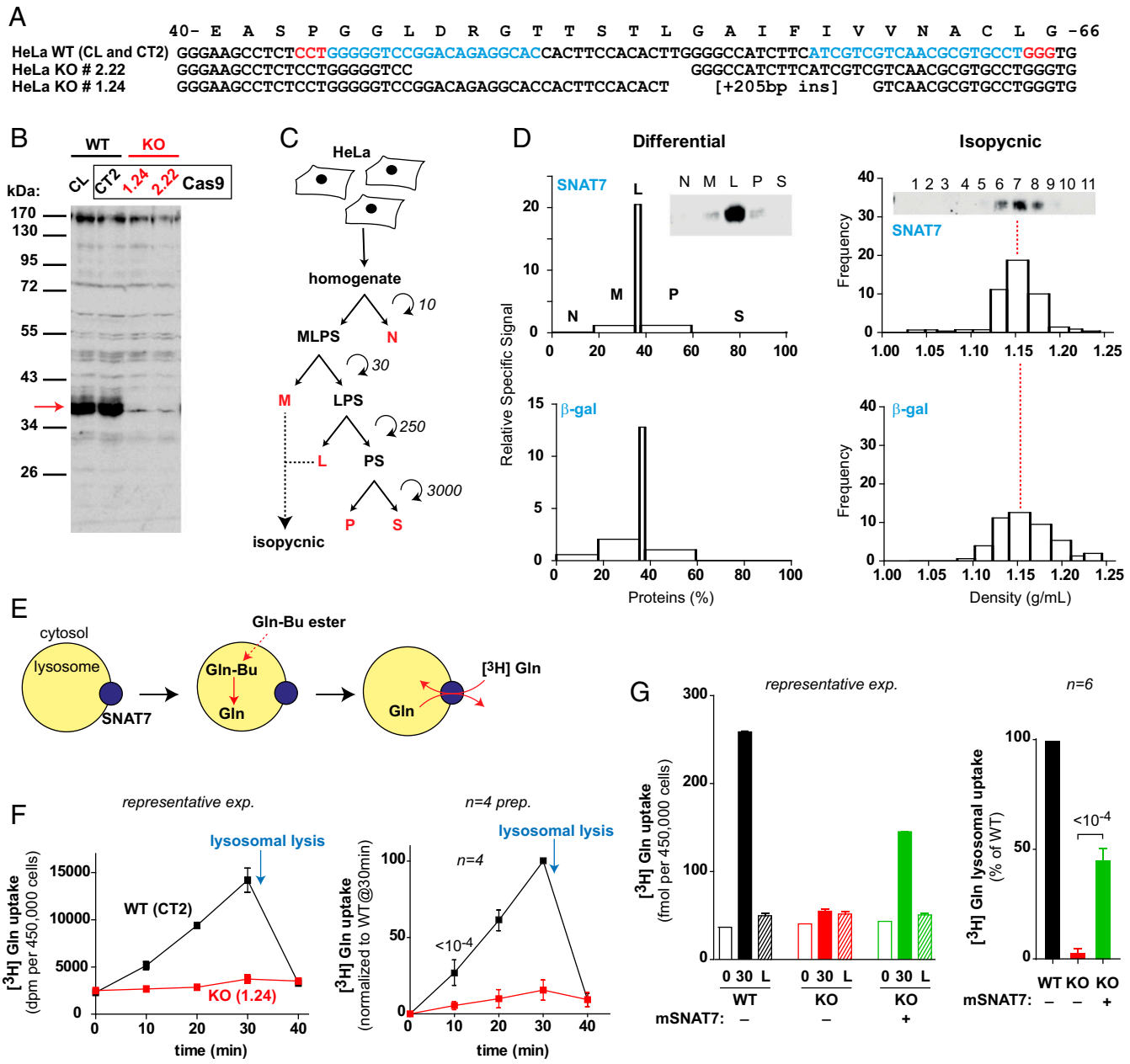

Fig. 2. SNAT7 is the major lysosomal transporter for glutamine and asparagine. (*A*) Genomic sequences of SNAT7 KO HeLa cell clones generated by the CRISPR/Cas9 method. The WT protein sequence of the targeted region is shown at the top. Protospacer adjacent motif (PAM) sequences are indicated in red, and target specific guide sequences are indicated in blue. The two KO clones display homozygous disruption of the *SLC38A7* gene: a 26-bp deletion and a 19-bp deletion + 205-bp insertion (ins) for clones 2.22 and 1.24, respectively. The control clone (CT2) shows no modification relative to the HeLa cell line (CL). (*B*) Characterization of the anti-hSNAT7 antibody by Western blot. SNAT7 appears as a strong 40-kDa band (red arrow) detected in lysates from WT, but not KO, HeLa cells. (*C*) Scheme for subcellular fractionation of HeLa cells. Centrifugation is expressed as 1,000 × *g* × min. L, light mitochondrial fraction; M, heavy mitochondrial fraction; N, nuclear fraction; P, peroxisomal and microsomal fraction; S, soluble fraction; MLPS, LPS and PS, supernatants containing the corresponding fractions. (*D*) Fractions from differential and isopycnic centrifugations were analyzed for SNAT7 immunoreactivity and for diverse organellar markers by Western blot and enzymatic measurements, respectively. Equal protein amounts were loaded on each lane of the blots shown. β-Galactosidase was used as a lysosomal marker (other cell compartments are shown in Fig. S3). For the differential centrifugation, graphs show the enrichment factor (Relative Specific Signal) of the protein of interest against the percentage of total proteins recovered in each fraction. For isopycnic centrifugation, the frequency (*Materials and Methods*) of the protein of interest is plotted against sucrose density. (*E*) Principle of the countertransport assay of SNAT7. Lysosomes partially purified from HeLa cells are selectively loaded with glutamine using glutamine-tert-butyl (Gln-Bu) ester. After washing, fractions are incubated with [^{3}H]Gln, which accumulates into lysosomes in exchange for intralysosomal glutamine. (*F*) SNAT7 mediates lysosomal countertransport of glutamine. Lysosome-enriched fractions, prepared from WT (CT2 clone, black squares) or SNAT7 KO (clone 1.24, red squares) HeLa cells, were preloaded with Gln, washed, and incubated with [^{3}H]Gln for diverse durations. [^{3}H]Gln uptake, determined by filtration and scintillation counting, increased linearly over time in a SNAT7-dependent manner. This uptake occurred in lysosomes as lysosomal lysis induced by 10 mM GME (arrow) released the radioactivity. A representative experiment (exp.; *Left*) and average normalized kinetics from four lysosome preparations (prep.; *Right*) are shown. *P* value is shown only for the earliest time point. (*G*) [^{3}H]Gln countertransport was assayed in fractions from WT HeLa cells (black) or SNAT7 KO clones transiently expressing (green), or not (red), mEGFP-SNAT7. Uptake was measured in triplicates at 0 min (open bars) or 30 min before (solid bars) or after (hatched bars) lysosomal lysis. Overexpression of mSNAT7 partially rescued glutamine uptake in SNAT7 KO lysosomes. A representative experiment (*Left*, mean ± SD of triplicate measurements) and average normalized values from six independent experiments performed on distinct lysosome preparations (*Right*) are shown.

However, mutation of the candidate sorting motifs tested (21-ERARLL-26 and 115-YQEV-118, mouse sequence numbering), either alone or in combination, did not alter SNAT7 localization.

We, thus, studied SNAT7 activity in isolated lysosomes by the ester loading/countertransport technique used in the 1980s to characterize most lysosomal amino acid transport activities (32). In this approach, lysosomes from a crude subcellular fraction are selectively loaded with a specific amino acid using an ester precursor, similar to the approach used above in our TFEB-based assay. Amino acid-loaded and unloaded lysosomes are then incubated with a radiolabeled free amino acid to measure their capacity to accumulate the radiotracer. Although most lysosomal amino acid transporters export their substrate from the organelle under physiological conditions, they accumulate the external amino acid in exchange for the internal one in this artificial setting (Fig. 2*E*) owing to a hallmark property of transporters known as transstimulation. This property directly results from the alternating-access mechanism of secondary transporters (33). Indeed, transporters operate by alternately exposing their substrate-binding site to one or the other side of the membrane. Under normal conditions, the transporter visits the whole set of inward/outward conformations and empty/loaded binding states. However, when lysosomes are artificially loaded with a high-substrate concentration, the inward and outward empty states can be bypassed, with the transporter thus shuttling back and forth between the two substrate-loaded conformations to exchange internal amino acids for the external radiotracer (Fig. 2*E*). Such artificially induced exchange reaction is called "countertransport."

To test whether this countertransport technique could detect the transport activity of SNAT7, we prepared a HeLa cell fraction enriched in lysosomes and preloaded these organelles with glutamine using glutamine-tert-butyl ester. After washing, fractions were incubated with L-[^{3}H]glutamine and the radioactivity accumulated into membrane vesicles was measured using a filtration assay. [^{3}H]Glutamine accumulated linearly over time into glutamine-loaded, but not glutamine-empty, fractions from WT HeLa cells and control Cas9 clones (Fig. 2*F* and Fig. S4*A*). Remarkably, inactivation of *SLC38A7* by genome editing decreased this countertransport by ∼90%, showing that it is carried by native SNAT7. To confirm that the observed [^{3}H]glutamine accumulation was contributed by lysosomes, 10 mM glycine methyl ester (GME), a concentration causing a selective osmotic stress and disruption of lysosomes (34), was added at the end of the uptake period. In agreement with the lysosomal localization of SNAT7, this treatment fully released the [^{3}H]glutamine accumulated into WT and control cellular fractions (Fig. 2 *F* and *G*). We considered the possibility that SNAT7-negative lysosomes might have lost their countertransport signal because they spontaneously rupture in our assay. To test this hypothesis, we exposed WT and knockout (KO) lysosomes to increasing concentrations of GME and assayed them for disruption using lysosomal enzyme release measurement. WT and KO lysosomes showed identical vulnerability to GME (Fig. S4*B*), thus ruling out this possibility.

To confirm that the glutamine transport activity was associated with SNAT7, we transiently expressed the mouse protein in KO HeLa cells. Mouse SNAT7 (mSNAT7) expression restored a robust [^{3}H]glutamine countertransport signal in these fractions (Fig. 2*G*). We concluded that SNAT7 is necessary and sufficient for lysosomal glutamine transport and that it represents the main glutamine permeation pathway across the lysosomal membrane. It may be noted that, to the best of our knowledge, lysosomal glutamine transport has not been reported thus far.

Next, we took advantage of the assay to characterize the transport properties of SNAT7. To examine its substrate selectivity, we tested glutamine-loaded fractions from WT and KO HeLa cells for their capacity to accumulate diverse tritiated amino acids. Again, selective lysosomal lysis with GME was used to discriminate the contributions of lysosomes and contaminating organelles. In agreement with our TFEB assay data, among the tested amino acids, only [^{3}H]glutamine and [^{3}H]asparagine accumulated into artificially loaded lysosomes in a SNAT7-dependent manner (Fig. 3*A* and Fig. S5). Our results thus strongly diverge from the broad amino acid selectivity reported by Hägglund et al. (30). In particular, we could not detect any uptake of [^{3}H]arginine (Fig. S5), which gave the most significant ($P < 0.001$) uptake signal in that study. It should be noted that [^{3}H]histidine was not transported in our assay (Fig. 3*A*), thus distinguishing SNAT7 from system N transporters within the SLC38 family.

These experiments informed us about the substrate selectivity on the cytosolic side of SNAT7. To test the selectivity on the luminal side, we compared the transstimulation properties of diverse amino acids by treating HeLa cell fractions with distinct esters before [^{3}H]glutamine countertransport measurement. Again, only asparagine and glutamine, but not alanine, glutamate, or serine, transstimulated [^{3}H]glutamine uptake (Fig. 3*B*). We concluded that SNAT7 is highly selective for asparagine and glutamine, in contrast to characterized members of the SLC38 family. Both amino acids seem to be translocated with similar efficiencies because their *cis* and *trans* effects were highly similar in these experiments (Fig. 3 *A* and *B*).

Finally, we examined the bioenergetics properties of SNAT7. Removal of ATP or inhibition of the V-type H^+-ATPase using bafilomycin A1 abolished [^{3}H]glutamine countertransport (Fig. 3*C*), suggesting that although the countertransport assay does not probe a full transport cycle, the lysosomal V-type H^+-ATPase is required for these partial reactions. To confirm and characterize the role of the V-ATPase, we applied ionophores in the presence of ATP to disrupt, or alter, the lysosomal proton electrochemical gradient. The proton ionophore carbonyl cyanide-4-(trifluoromethoxy)phenylhydrazone (FCCP), which fully disrupts this gradient, abolished [^{3}H]glutamine countertransport (Fig. 3*D*). Valinomycin, a potassium ionophore that disrupts the electrical component of the gradient (membrane potential) but preserves the pH gradient, had no effect. In contrast, nigericin, an H^+/K^+ exchanger that disrupts the pH gradient but preserves the membrane potential, abolished [^{3}H]glutamine countertransport (Fig. 3*D*). These data show that the acidic milieu of lysosomes is required to activate SNAT7. A potential explanation may be that amino acid transport by SNAT7 is coupled to proton, thus requiring protonation from the lysosomal lumen to perform the partial transport reaction measured in our assay.

Taken together, our TFEB-based live-cell assay and our countertransport measurements indicate that SNAT7 is an amino acid transporter highly selective for glutamine and asparagine and that it represents the primary export pathway for these amino acids across the lysosomal membrane.

SNAT7 Is Required for Extracellular Protein-Dependent Proliferation of Cancer Cells in a Low Free-Glutamine Environment. Cancer cells require a high level of glutamine for rapid proliferation and survival. When the extracellular environment does not meet their needs, several types of cancer use opportunistic cell-nutrition routes, including macropinocytosis of extracellular proteins, phagocytosis of apoptotic corpses, or entosis (cell "cannibalism") to acquire amino acids (11). In particular, macropinocytosis of extracellular proteins is an essential glutamine supply route for the growth of Ras-transformed cells (12). These opportunistic cell-nutrition routes converge onto the lysosome and, consequently, onto lysosomal amino acid exporters. The demonstration that SNAT7 is the primary lysosomal glutamine transporter thus prompted us to examine whether it is required for extracellular protein-dependent growth of cancer cells.

We examined this hypothesis using the MIA PaCa-2 cell line, derived from a human pancreatic adenocarcinoma, which harbors

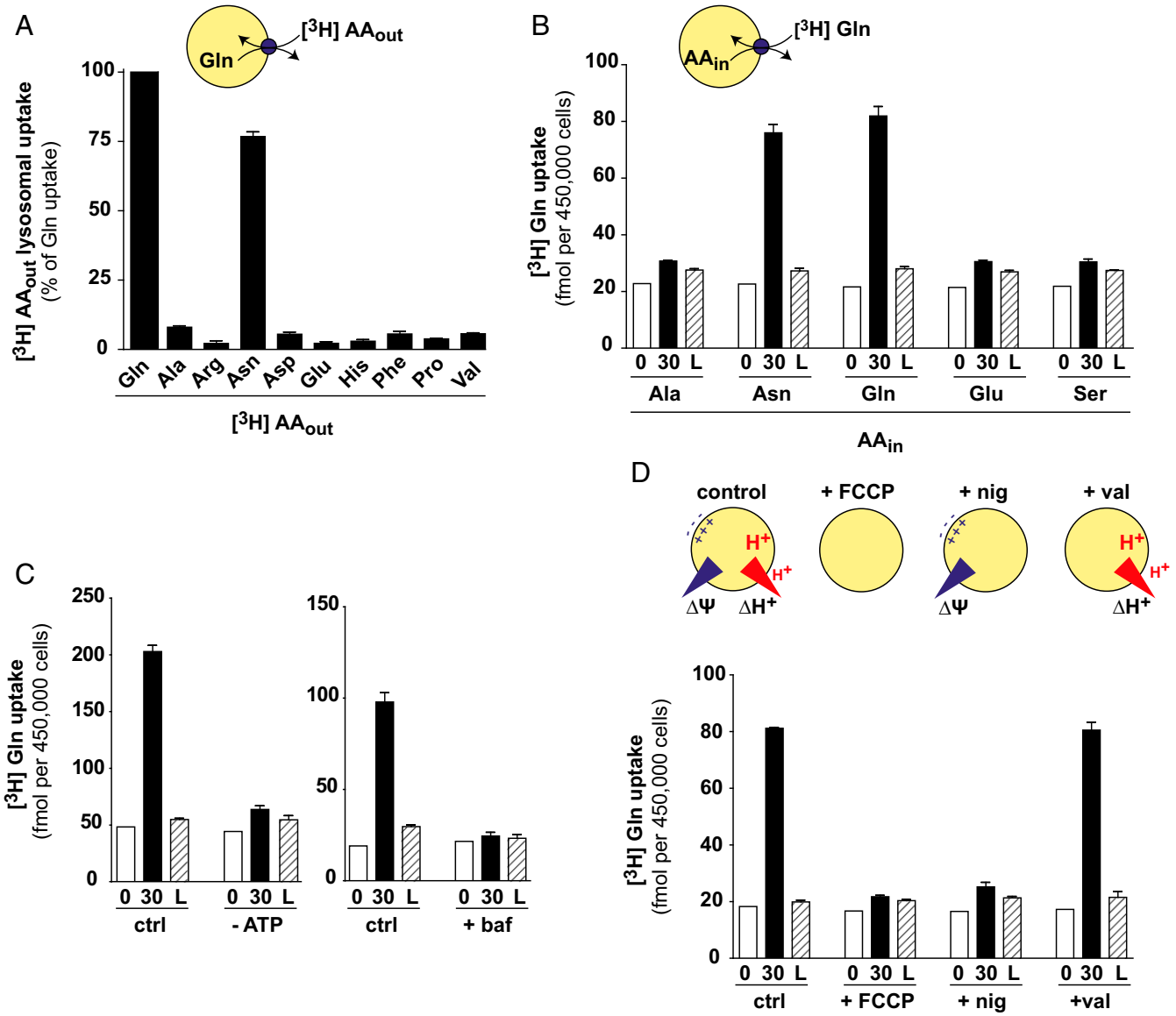

Fig. 3. Functional properties of SNAT7. (*A*) Substrate selectivity on the cytosolic side. Lysosome-enriched fractions from WT and SNAT7 KO HeLa cells were preloaded with glutamine and assayed for countertransport of various [^{3}H]AA for 30 min. Specific lysosomal uptake, determined based on GME-induced lysis and SNAT7 dependence (*Materials and Methods*), was calculated for each substrate and normalized to the [^{3}H]Gln signal. (*B*) Substrate selectivity on the luminal side. [^{3}H]Gln countertransport was assayed in lysosome-enriched fractions preloaded with various amino acids using ester precursors. (*C*) [^{3}H]Gln countertransport was assayed as in *A* (ctrl) and either in the absence of ATP (*Left*) or in the presence of 500 nM bafilomycin A1 (baf; *Right*). (*D*) Lysosomal v-ATPase creates an electrochemical H^+ gradient (acidic and positive inside) across the lysosomal membrane. Ionophores can selectively disrupt the chemical [pH gradient (ΔpH)] or electrical component [voltage gradient (ΔΨ)], or both, as depicted in the scheme. The [^{3}H]Gln countertransport was assayed as in *A* in the presence of ATP and 3 μM nigericin (nig), valinomycin (val), or FCCP. Disruption of the pH gradient, but not the voltage gradient, abolished [^{3}H]Gln uptake. The graph in *A* shows mean values from two independent experiments. Other graphs are representative experiments of two (*B* and *D*) or three (*C*) experiments performed on distinct lysosome preparations. Error bars represent SD from triplicate measurements.

homozygous activating mutations in the Kirsten rat sarcoma viral oncogene homologue (*KRAS*) gene (35). In agreement with Commisso et al. (12), we observed that MIA PaCa-2 cell growth depends on extracellular free glutamine and that BSA supplementation helps cells grow at low, but not high, free-glutamine concentrations (Fig. 4*A*). In contrast, supplementation of the medium (which lacks asparagine) with 1 mM asparagine did not rescue cell growth at a low free-glutamine concentration (0.05 mM), showing that asparagine cannot compensate for the loss of glutamine. To evaluate the role of SNAT7 in this BSA-dependent growth, we silenced the *SLC38A7* gene in MIA PaCa-2 cells using three Dicer-substrate short interfering RNAs (DsiRNAs) targeting hSNAT7 (S7-1, S7-2, and S7-3; TriFECTa RNAi kit; Integrated DNA Technologies) or, as negative controls, a DsiRNA with no target sequence in the human genome (CT-1) and a DsiRNA targeting hypoxanthine phosphoribosyltransferase 1 (CT-2). Individual treatment with each SNAT7-targeted DsiRNA strongly reduced the hSNAT level upon immunoblotting analysis (Fig. 4*B*). We thus tested the effect of BSA on the growth of DsiRNA-treated MIA PaCa-2 cells at a low free-glutamine concentration (0.2 mM). BSA supplementation (2%) increased the growth of control cells by 55% over 5 d. In contrast, this effect was reduced to 18–25% in *SLC38A7*-silenced cells (Fig. 4*B*). SNAT7 is, thus, required by these pancreatic cancer cells to use

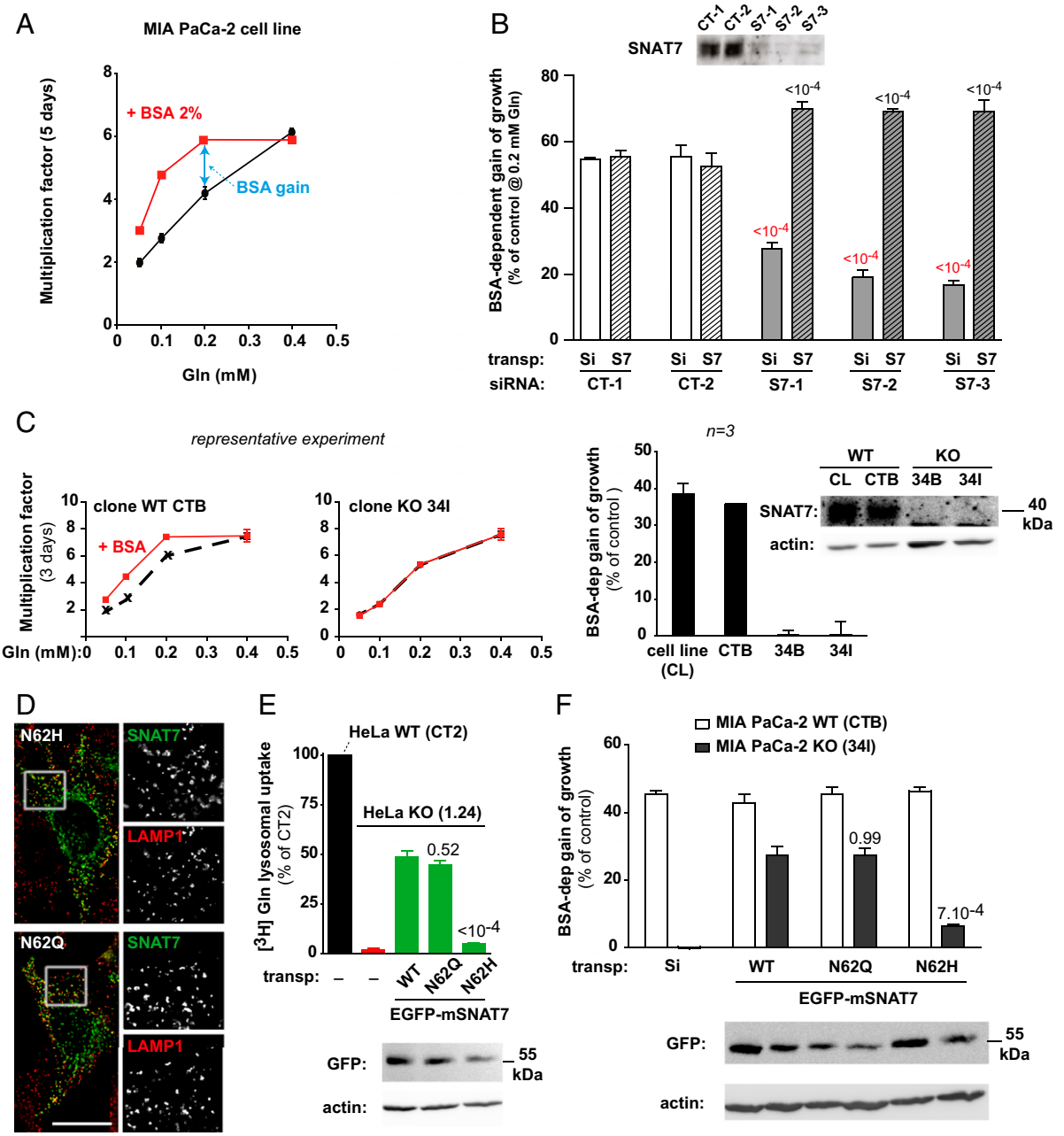

Fig. 4. SNAT7 transport activity is required for extracellular protein-dependent growth of cancer cells in a low free-glutamine environment. (*A*) BSA supplementation (2%) rescues MIA PaCa-2 cell growth in low free-glutamine medium. Growth was measured in triplicate at diverse Gln concentrations by cell counting and expressed as the mean ratio ± SD between final and initial cell numbers. One representative experiment of three is shown. (*B*) SNAT7 expression was silenced in MIA PaCa-2 cells using three distinct *SLC38A7*-targeted siRNAs (S7-1, S7-2, and S7-3) or two control siRNAs (CT-1 and CT-2) as negative controls. (*Inset*) *SLC38A7* silencing strongly reduced SNAT7 expression (Western blot). Cells were then transiently transfected with mSNAT7 (S7) or, as a negative control, a nontransporting sialin construct (Si) and assayed for 2% BSA-dependent growth at 0.2 mM Gln (double arrow in *A*). SNAT7 silencing decreased, and mSNAT7 expression rescued, BSA-dependent growth. The graph shows mean value ± SD from three independent experiments. *P* values for the difference between control (white bars) and siRNA-treated (gray bar) samples and between siRNA-treated (gray bar) and mSNAT7-reexpressing (gray hatched bar) samples are displayed in red and black, respectively. (*C*) SNAT7 expression was abolished in MIA PaCa-2 cells using CRISPR/Cas9 gene editing. The resulting clones were assayed for BSA-dependent growth as in *A*. (*Left* and *Center*) Graphs show a representative experiment for a WT clone (CTB) and a KO clone (34I) with (red curve) or without (black) BSA at diverse Gln concentrations. (*Right*) Graph shows mean BSA-dependent growth value ± SD for three independent experiments at 0.2 mM Gln for the cell line, one control clone (CTB), and two independent KO clones (34B and 34I). (*Inset*) Loss of SNAT7 expression was verified by Western blot. (*D*, *Left*) Fluorescence micrographs of HeLa cells expressing N62H and N62Q mEGFP-SNAT7 (green) show a good overlap with the lysosomal marker LAMP1 (red). (*D*, *Right*) Magnifications (2.5×) of the selected areas are shown for each channel. (Scale bar: 20 μm.) (*E*) Rescue experiments of [^{3}H]Gln countertransport in HeLa cells. Uptake was assayed in fractions from WT cells (black); SNAT7 KO cells (red, 1.24 clone); and KO cells transiently expressing WT, N62Q, or N62H mEGFP-SNAT7 (green) as in Fig. 2*F*. The graph shows mean ± SD values normalized to WT cells from three independent experiments. *P* values relative to WT-expressing KO cells are indicated above the bars. The expression of EGFP-mSNAT7 was checked by Western blot. (*F*) Rescue experiments of BSA-dependent growth in MIA PaCa-2 cells. WT (white bars) and KO (black) clones transiently expressing sialin (Si) or the indicated mEGFP-SNAT7 constructs were assayed for 2% BSA-dependent growth in 0.2 mM Gln over 3 d. WT and N62Q mSNAT7 rescue BSA-dependent growth, in contrast to the transport-defective N62H mutant. The graph shows mean ± SD values from three independent experiments. *P* values relative to WT-expressing KO cells are indicated above the bars. The expression of EGFP-mSNAT7 was checked by Western blot.

BSA for growth in low free-glutamine medium. A similar effect of SNAT7 was observed with the human ovarian carcinoma A2780 cell line (Fig. S6*B*).

To test whether SNAT7 gene silencing affected the BSA-dependent nutrition route at steps upstream of lysosomal glutamine export, we used the fluorogenic probe DQ-Red-BSA, which enables monitoring the internalization and lysosomal degradation of BSA. DQ-Red-BSA is highly conjugated with a fluorophore that, after uptake by fluid-phase endocytosis or macropinocytosis, undergoes dequenching on lysosomal proteolysis. *SLC38A7* silencing did not alter the capacity of MIA PaCa-2 cells to internalize and degrade DQ-Red-BSA (Fig. S6*C*), implying that SNAT7 is involved downstream of lysosomal proteolysis (i.e., owing to its location and molecular function) at the lysosomal export step.

To confirm the dependence of BSA-dependent cell growth on SNAT7, we inactivated the *SLC38A7* gene in MIA PaCa-2 cells using the CRISPR/Cas9 nickase method. The loss of SNAT7 in selected MIA PaCa-2 cell clones was confirmed by genomic sequencing and immunoblotting (Fig. 4*C* and Fig. S7). Remarkably, BSA-dependent growth was fully abolished in clones carrying two loss-of-function *SLC38A7* mutations, but not in control (unedited) clones (Fig. 4*C*).

Finally, we performed rescue experiments to confirm the role of SNAT7 in BSA-dependent growth under restricted glutamine availability and to test whether this role involves its transport activity. Transient expression of mSNAT7, which is insensitive to the hSNAT7-targeted DsiRNAs, rescued BSA-dependent growth of MIA PaCa-2 cells under low free glutamine to 69% (Fig. 4*B*). Similarly, mSNAT7 rescued the BSA-dependent growth of MIA PaCa-2 cell clones to 23% (Fig. 4*F*). To examine whether SNAT7 promotes BSA-dependent growth through its amino acid transport function, we tested the effect of mutations that impact this function. A highly conserved asparagine present in the first transmembrane domain of SLC38 transporters plays a critical role in amino acid transport (36, 37). Mutation of this residue (N62) to glutamine or histidine did not affect the lysosomal localization of transfected mSNAT7 (Fig. 4*D*). The mutant proteins were, thus, expressed in HeLa clones devoid of hSNAT7 to assess their transport activity. Interestingly, N62H strongly reduced lysosomal glutamine countertransport (10 ± 3% of WT mSNAT7 signal, $n = 3$), whereas the conservative mutation N62Q fully preserved this activity (Fig. 4*E*). In excellent agreement with these data, N62Q mSNAT7 rescued the BSA-dependent growth of MIA PaCa-2 cells lacking hSNAT7 as efficiently as the WT protein, whereas the N62H mutation had little effect (only 23 ± 4% of WT mSNAT7-induced growth, $n = 3$) (Fig. 4*F*). The role of SNAT7 in extracellular protein-dependent growth, thus, clearly correlates with its amino acid transport activity.

Taken together, our results show that SNAT7 is the primary export pathway of glutamine and asparagine from the lysosome and that its transport activity is essential to supply extracellular protein-derived glutamine to cancer cells when free glutamine is at an insufficient level in their environment.

Discussion

In this study, we provide biochemical and functional evidence for the lysosomal localization of native SNAT7, thus strengthening our former proteomic (native SNAT7) and fluorescence microscopy (GFP-tagged SNAT7) evidence (19). First, in HeLa cells submitted to two different subcellular fractionation methods (differential and isopycnic centrifugations), native SNAT7 mainly codistributes with a lysosomal marker. Second, our countertransport assay combined with gene-editing experiments shows that the transport activity of SNAT7 is affected by prior incubation with amino acid esters, a treatment known to load selectively or, at high concentration, to disrupt lysosomes in crude subcellular fractions (32). Finally, this transport activity requires an acidic lysosomal lumen, implying that SNAT7 is not active before its delivery to endosomes and lysosomes, and that a minor presence, if any, of SNAT7 at the plasma membrane should not significantly contribute to amino acid homeostasis in cells living in a neutral environment. It should be stressed that although luminal acidity stimulated lysosomal [^{3}H]glutamine uptake under the artificial conditions of our countertransport assay, our in situ TFEB-based assay clearly shows that SNAT7 operates in the export direction in live cells. A very recent proteomic study of multiple subcellular compartments from rat liver also identified lysosomes as the major, if not exclusive, cellular location of SNAT7 (38).

We also provide a detailed characterization of the transport activity of SNAT7. In particular, we show both in an indirect live-cell assay and in direct flux measurements that SNAT7 is highly selective for glutamine and asparagine, in marked contrast to the broad amino acid selectivity reported by an earlier study (30). The most likely reason for this discrepancy is the very low background-level signals observed with the whole-cell *Xenopus* oocyte assay used by Hägglund et al. (30), which did not provide reliable signals in our attempts to replicate these data.

Moreover, our gene knock-down and KO experiments indicate that, at least in two cell types, SNAT7 is the primary permeation pathway for glutamine (HeLa and Mia PACA-2) and asparagine (HeLa) across the lysosomal membrane. Therefore, although other candidate lysosomal glutamine transporters have been reported (15, 16, 19), their contribution may be negligible or restricted to specific cell types with low SNAT7 levels. SNAT4, a neutral amino acid transporter (39), has been detected in the liver lysosomal membrane with a high spectral index, a parameter reflecting a strong association with lysosome-enriched fractions, in our earlier proteomic study (19). However, its transport activity at the plasma membrane requires an alkaline extracellular pH, with no detectable activity at pH ≤ 6 (39), in contrast to the strong acidity of the topologically equivalent lysosomal lumen. The presence of SNAT4 in liver lysosomes may thus reflect its abundance in this tissue and its turnover in the endocytosis pathway, rather than an active transport role at the lysosomal membrane. SNAT9 is another SLC38 protein found in the lysosome, which participates in the amino acid-sensing machinery that regulates mTORC1 at the lysosomal surface (15, 16, 18). Flux measurements in reconstituted liposomes showed that SNAT9 transport activity has a broad selectivity for amino acids, including glutamine and asparagine (15, 16). However, the transport activity measured in this assay was extremely slow (15, 16), suggesting that SNAT9 may act as a transceptor (17) rather than a bona fide transporter. Moreover, the functional interaction of SNAT9 with mTORC1 indicates a selective role in transmitting arginine levels, rather than the levels of other amino acids, to mTORC1 (16). The presence of SNAT9 in the lysosomal membrane thus does not challenge our conclusion that SNAT7 is the predominant lysosomal transporter for asparagine and glutamine.

Conversely, because SNAT7 belongs to the same protein family as SNAT9, it may be asked whether SNAT7 can act as a transceptor signaling amino acid levels to mTORC1 in addition to its bona fide transport function. Two lines of evidence argue against such a possibility. First, alignment of the SNAT7 and SNAT9 amino acid sequences (Fig. S8) shows that SNAT7 lacks a large part of the N-terminal cytosolic domain responsible for the physical interaction of SNAT9 with the Ragulator complex and the Rag GTPases that recruit mTORC1 to the lysosomal surface (15, 16, 18). Moreover, five of six identified residues that are critical for this interaction (16) are not conserved in the SNAT7 sequence (Fig. S8). Second, Ragulator or Rag pull-down experiments do not precipitate SNAT7, in contrast to SNAT9 (15). Therefore, although the two lysosomal SLC38 transporters both contribute to intracellular amino acid homeostasis, they seem to play quite distinct roles in either amino acid sensing (SNAT9) or the supply of cytosolic amino acids (SNAT7) derived from intracellular (autophagy) and extracellular (macropinocytosis and phagocytosis) stores.

Metabolic reprogramming is a hallmark of cancer cells, and it is required for both oncogenic transformation and tumor development (11, 40). In addition to the well-known Warburg effect, this metabolic reprogramming includes an increased consumption of glutamine, which is used as a nitrogen donor for nonessential amino acid and nucleobase synthesis and as a carbon donor to replenish TCA cycle intermediates (anaplerosis) for energy production and cellular redox homeostasis (11, 40, 41). Consequently, many cancer cells are addicted to glutamine. Glutamine is usually supplied as a free amino acid by the blood flow, but when the vasculature is compromised, as in the tumor core, cancer cells have evolved alternative strategies to acquire amino acids, including macropinocytosis and lysosomal degradation of extracellular proteins as observed, for instance, in pancreatic ductal adenocarcinoma (11, 12, 42). Our study extends this picture by identifying SNAT7 as a key protein supplying extracellular protein-derived glutamine into the cytosol.

Ras-activating mutations are known to stimulate macropinocytotic uptake of extracellular proteins (12, 42, 43), thus explaining the key role of SNAT7 in the extracellular protein-dependent growth of MIA PaCa-2 cells (Fig. 4). Macropinocytosis is also stimulated by Src-activating mutations (44). Surprisingly, although A2780 cells do not carry such mutations, they also use extracellular proteins in a SNAT7-dependent manner to grow in low free-glutamine medium (Fig. S6*B*), albeit to a lesser extent than MIA PaCa-2 cells. This finding suggests that internalization of extracellular proteins and SNAT7-mediated supply of protein-derived glutamine may have a broader significance than generally anticipated, with either strong or partial dependence on this nutrition pathway depending on its relative level compared with glutamine biosynthesis. Inhibiting SNAT7 may thus provide a novel type of anticancer therapy for Ras-activated, Src-activated, and possibly other types of cancers characterized by an increased consumption of glutamine and poorly vascularized tumors.

Although SNAT7 efficiently exports both glutamine and asparagine from the lysosome, the dependence of extracellular protein-dependent growth on SNAT7 is most probably associated with its glutamine export activity because asparagine does not rescue MIA PaCa-2 cell growth in low free-glutamine medium. This selective dependence of cell growth on glutamine supply may arise from the hub-like role of this amino acid in mammalian cell metabolism. Indeed, glutamine is a precursor for several important metabolic pathways (nucleotide, hexosamine, and glutathione synthesis and replenishment of Krebs cycle intermediates) in addition to protein synthesis. Moreover, in mammals, the nitrogen donor for asparagine synthesis is glutamine instead of ammonia. Therefore, asparagine biosynthesis depends on glutamine, but the converse is not true.

Interestingly, the pathogenesis of pancreatic ductal adenocarcinoma also involves a transcriptional program, which is induced by constitutive activation of TFEB and related transcription factors (MITF, TFE3), and which up-regulates autophagy and lysosomal biogenesis to maintain intracellular amino acid pools under conditions of nutrient deprivation, thereby promoting cell survival (45). If glutamine availability significantly contributes to this survival response, for instance, by maintaining the cellular redox balance (41), inhibiting SNAT7 might trigger cell death, in addition to preventing macropinocytosis-dependent growth, because of the key role of lysosomes at the intersection of the macropinocytosis and autophagy pathways. The role of SNAT7 as a primary route for (auto)lysosomal glutamine export thus makes it an attractive potential therapeutic target for this extremely aggressive type of cancer.

Materials and Methods

Cell Culture and DNA Transfection. Human cell lines were used in accordance with the regulations and guidelines from the French Ministry of Higher Education and Research (CODECOH). HeLa, A2780, and Mia-PaCa2 cells were grown in DMEM supplemented with 10% FBS, 50 $\mu g \cdot mL^{-1}$ streptomycin, and 50 $U \cdot mL^{-1}$ penicillin ("complete medium"; all products from GIBCO). They were kept in a humidified atmosphere at 37 °C with 5% CO_2. For CRISPR/Cas9 genome edition and rescue experiments, HeLa and Mia-PaCa2 cells were transfected using Lipofectamine 2000 (Thermo Fisher Scientific) and Lullaby (OzBiosciences), respectively, according to the manufacturers' instructions. For the TFEB-based and countertransport assays of lysosomal transporters, HeLa cells were transfected by electroporation as described elsewhere (9).

TFEB-Based Assay of Lysosomal Amino Acid Transport. HeLa cells were electroporated with two plasmids, one encoding mRFP-hTFEB and another encoding a lysosomal transporter: EGFP-mSNAT7, EGFP-LYAAT1, rPQLC-EGFP (25), or EGFP-sialin P334R (9). They were then seeded onto coverslips in 24-well plates (160,000 cells per well) and grown for 48 h. Cells were then treated for 2 h at 37 °C in complete culture medium supplemented with 25 mM Hepes (pH 7.4) and the following amino acid esters: 3 mM alanine methyl-ester, 10 mM aspartate dimethyl-ester, 4.5 mM glycine methyl-ester, 40 mM lysine methyl-ester, 1.7 mM leucine methyl-ester, 6 mM methionine methyl-ester, 27 mM asparagine methyl-ester, 3.75 mM glutamine tert-butyl-ester, 7 mM serine methyl-ester, 1 mM tryptophan methyl-ester, and 3.7 mM tyrosine methyl-ester (all from Sigma, except glutamine tert-butyl-ester from Santa Cruz Biotechnology). Cells were then washed in PBS^{++} (supplemented with 0.1 mM $CaCl_2$ and 0.1 mM $MgCl_2$), fixed with 4% paraformaldehyde, washed in 50 mM NH_4Cl, and rinsed in PBS^{++}, before mounting coverslips onto glass slides using Fluoromount-G (Southern Biotech). Cells were first visualized under epifluorescence microscopy in the green channel to select at least four different fields and 50 transporter-expressing cells for each condition and then visualized in the red channel to determine and categorize (Fig. 1*B*) the distribution of mRFP-hTFEB. In proof-of-concept experiments, samples were categorized identically by two independent observers.

Countertransport Measurements. Lysosome-enriched fractions were prepared from HeLa cells at 4 °C essentially as described elsewhere (46), using pipette tips cut obliquely to minimize lysosome breakage. A total of 22.5×10^6 cells were harvested with trypsin, washed, and resuspended in 1.1 mL of purification buffer (250 mM sucrose, 10 mM acetic acid, 10 mM ethanolamine, 2.5 mM KCl, 1 mM EDTA, and 5 mM ATP adjusted to pH 7.4 with NaOH). Cells were broken by 50 passages through a 27-gauge × 3/4 needle and centrifuged at 750 × *g* for 10 min. The supernatant was kept, and the pellet resuspended in 1.1 mL of purification buffer was centrifuged again at 750 × *g* for 10 min. The two supernatants were pooled and centrifuged at 1,500 × *g* for 15 min, and the resulting supernatant was centrifuged at 20,000 × *g* for 15 min. The resulting pellet was resuspended in 110 μL of purification buffer supplemented with amino acid esters (same concentrations as in the TFEB-based assay) and incubated at 25 °C for 15 min. The mix was split into four tubes of 25 μL and centrifuged at 20,000 × *g* for 15 min. Each pellet was resuspended in 400 μL of purification buffer supplemented with 4 μCi of ^{3}H-amino acid (PerkinElmer; final concentration 200 nM). When mentioned, 3 μM nigericin, FCCP, or valinomycin (all from Sigma) was added. Mixes were then split into seven hemolysis tubes (50 μL per tube) kept on ice. One mix was directly filtered (discussed below) to determine background radioactivity. The six remaining mixes were incubated at 25 °C for 30 min. Three of them were immediately filtered, whereas three others were incubated further for 10 min in the presence of 10 mM glycine-methyl-ester specifically to disrupt the lysosomes before filtration. The accumulated radioactivity was determined by diluting mixes with 3 mL of chilled PBS and filtration onto a 0.45-μm pore nitrocellulose membrane (HAWP02500; Millipore), followed by three washes with chilled PBS. The radioactivity retained on filters was determined using a Tri-Carb 2100 TR liquid scintillation analyzer (Packard). In Fig. 3*A*, specific lysosomal uptake, determined based on GME-induced lysis and SNAT7 dependence, was calculated as $(\text{uptake @ 30 min} - \text{uptake after lysosomal lysis})_{WT} - (\text{uptake @ 30 min} - \text{uptake after lysosomal lysis})_{KO}$.

Growth Assays. At day 1, MIA PaCa-2 or A2780 cells were seeded in 24-well plates at 15,000 or 60,000 cells per well in DMEM without glutamine supplemented with penicillin, streptomycin, Hepes-Na^+ (pH 7.4) (25 mM) and dialyzed FBS (10%; Gibco). Medium was supplemented with various concentrations of glutamine (Sigma) and fatty acid-free BSA (reference no. 126609; Calbiochem) at the indicated concentrations. Medium was replaced at days 2 and 3. At day 4, cells were counted using an automatic cell counter (Beckman Coulter).

Statistics. One-way ANOVA with the post hoc Tukey's test was performed with GraphPad Prism. Additional information is provided in *SI Materials and Methods* (16, 28, 29, 47).

ACKNOWLEDGMENTS. We thank François Darchen for comments on the manuscript. We are grateful to Cécile Debacker, Stéphanie Dupuy, and Virginie Tevel for technical help in cell culture, flow cytometry, and fractionation experiments, respectively. This study was supported by Ligue contre le Cancer, Comité de Paris Grants RS15/75-82 and RS16/75-101 (to B.G.) and the CNRS. Q.V. was supported by PhD fellowships from the Ministère de l'enseignement supérieur et de la recherche (Doctoral School BIOSIGNE at Paris-Sud University) and from the charity Vaincre les Maladies Lysosomales. C.S. is a scientist from the Institut National de la Santé et de la Recherche Médicale.

1. Aits S, Jäättelä M (2013) Lysosomal cell death at a glance. *J Cell Sci* 126:1905–1912.
2. Andrews NW, Almeida PE, Corrotte M (2014) Damage control: Cellular mechanisms of plasma membrane repair. *Trends Cell Biol* 24:734–742.
3. Efeyan A, Comb WC, Sabatini DM (2015) Nutrient-sensing mechanisms and pathways. *Nature* 517:302–310.
4. Napolitano G, Ballabio A (2016) TFEB at a glance. *J Cell Sci* 129:2475–2481.
5. Rutsch F, et al. (2009) Identification of a putative lysosomal cobalamin exporter altered in the cblF defect of vitamin B12 metabolism. *Nat Genet* 41:234–239.
6. Coelho D, et al. (2012) Mutations in ABCD4 cause a new inborn error of vitamin B12 metabolism. *Nat Genet* 44:1152–1155.
7. Kawaguchi K, Okamoto T, Morita M, Imanaka T (2016) Translocation of the ABC transporter ABCD4 from the endoplasmic reticulum to lysosomes requires the escort protein LMBD1. *Sci Rep* 6:30183.
8. Bardor M, Nguyen DH, Diaz S, Varki A (2005) Mechanism of uptake and incorporation of the non-human sialic acid N-glycolylneuraminic acid into human cells. *J Biol Chem* 280:4228–4237.
9. Morin P, Sagné C, Gasnier B (2004) Functional characterization of wild-type and mutant human sialin. *EMBO J* 23:4560–4570.
10. Samraj AN, Läubli H, Varki N, Varki A (2014) Involvement of a non-human sialic Acid in human cancer. *Front Oncol* 4:33.
11. Pavlova NN, Thompson CB (2016) The emerging hallmarks of cancer metabolism. *Cell Metab* 23:27–47.
12. Commisso C, et al. (2013) Macropinocytosis of protein is an amino acid supply route in Ras-transformed cells. *Nature* 497:633–637.
13. Bröer S (2014) The SLC38 family of sodium-amino acid co-transporters. *Pflugers Arch* 466:155–172.
14. Hägglund MGA, et al. (2015) Transport of l-glutamine, l-alanine, l-arginine and l-histidine by the neuron-specific slc38a8 (SNAT8) in CNS. *J Mol Biol* 427:1495–1512.
15. Rebsamen M, et al. (2015) SLC38A9 is a component of the lysosomal amino acid sensing machinery that controls mTORC1. *Nature* 519:477–481.
16. Wang S, et al. (2015) Metabolism. Lysosomal amino acid transporter SLC38A9 signals arginine sufficiency to mTORC1. *Science* 347:188–194.
17. Thevelein JM, Voordeckers K (2009) Functioning and evolutionary significance of nutrient transceptors. *Mol Biol Evol* 26:2407–2414.
18. Jung J, Genau HM, Behrends C (2015) Amino acid-dependent mTORC1 regulation by the lysosomal membrane protein SLC38A9. *Mol Cell Biol* 35:2479–2494.
19. Chapel A, et al. (2013) An extended proteome map of the lysosomal membrane reveals novel potential transporters. *Mol Cell Proteomics* 12:1572–1588.
20. Sardiello M, et al. (2009) A gene network regulating lysosomal biogenesis and function. *Science* 325:473–477.
21. Settembre C, et al. (2012) A lysosome-to-nucleus signalling mechanism senses and regulates the lysosome via mTOR and TFEB. *EMBO J* 31:1095–1108.
22. Martina JA, Chen Y, Gucek M, Puertollano R (2012) MTORC1 functions as a transcriptional regulator of autophagy by preventing nuclear transport of TFEB. *Autophagy* 8:903–914.
23. Roczniak-Ferguson A, et al. (2012) The transcription factor TFEB links mTORC1 signaling to transcriptional control of lysosome homeostasis. *Sci Signal* 5:ra42.
24. Reeves JP (1979) Accumulation of amino acids by lysosomes incubated with amino acid methyl esters. *J Biol Chem* 254:8914–8921.
25. Jézégou A, et al. (2012) Heptahelical protein PQLC2 is a lysosomal cationic amino acid exporter underlying the action of cysteamine in cystinosis therapy. *Proc Natl Acad Sci USA* 109:E3434–E3443.
26. Sagné C, et al. (2001) Identification and characterization of a lysosomal transporter for small neutral amino acids. *Proc Natl Acad Sci USA* 98:7206–7211.
27. Liu B, Du H, Rutkowski R, Gartner A, Wang X (2012) LAAT-1 is the lysosomal lysine/arginine transporter that maintains amino acid homeostasis. *Science* 337:351–354.
28. Ran FA, et al. (2013) Genome engineering using the CRISPR-Cas9 system. *Nat Protoc* 8:2281–2308.
29. de Duve C, Pressman BC, Gianetto R, Wattiaux R, Appelmans F (1955) Tissue fractionation studies. 6. Intracellular distribution patterns of enzymes in rat-liver tissue. *Biochem J* 60:604–617.
30. Hägglund MG, et al. (2011) Identification of SLC38A7 (SNAT7) protein as a glutamine transporter expressed in neurons. *J Biol Chem* 286:20500–20511.
31. Kalatzis V, Cherqui S, Antignac C, Gasnier B (2001) Cystinosin, the protein defective in cystinosis, is a H(+)-driven lysosomal cystine transporter. *EMBO J* 20:5940–5949.
32. Pisoni RL, Thoene JG (1991) The transport systems of mammalian lysosomes. *Biochim Biophys Acta* 1071:351–373.
33. Drew D, Boudker O (2016) Shared molecular mechanisms of membrane transporters. *Annu Rev Biochem* 85:543–572.
34. Goldman R, Kaplan A (1973) Rupture of rat liver lysosomes mediated by L-amino acid esters. *Biochim Biophys Acta* 318:205–216.
35. Moore PS, et al. (2001) Genetic profile of 22 pancreatic carcinoma cell lines. Analysis of K-ras, p53, p16 and DPC4/Smad4. *Virchows Arch* 439:798–802.
36. Bröer S, Schneider H-P, Bröer A, Deitmer JW (2009) Mutation of asparagine 76 in the center of glutamine transporter SNAT3 modulates substrate-induced conductances and Na+ binding. *J Biol Chem* 284:25823–25831.
37. Zhang Z, Gameiro A, Grewer C (2008) Highly conserved asparagine 82 controls the interaction of Na+ with the sodium-coupled neutral amino acid. 283:12284–12292.
38. Jadot M, et al. (2017) Accounting for protein subcellular localization: A compartmental map of the rat liver proteome. *Mol Cell Proteomics* 16:194–212.
39. Hatanaka T, et al. (2001) Evidence for the transport of neutral as well as cationic amino acids by ATA3, a novel and liver-specific subtype of amino acid transport system A. *Biochim Biophys Acta* 1510:10–17.
40. Boroughs LK, DeBerardinis RJ (2015) Metabolic pathways promoting cancer cell survival and growth. *Nat Cell Biol* 17:351–359.
41. Son J, et al. (2013) Glutamine supports pancreatic cancer growth through a KRAS-regulated metabolic pathway. *Nature* 496:101–105.
42. Palm W, et al. (2015) The utilization of extracellular proteins as nutrients is suppressed by mTORC1. *Cell* 162:259–270.
43. Bar-Sagi D, Feramisco JR (1986) Induction of membrane ruffling and fluid-phase pinocytosis in quiescent fibroblasts by ras proteins. *Science* 233:1061–1068.
44. Veithen A, Cupers P, Baudhuin P, Courtoy PJ (1996) v-Src induces constitutive macropinocytosis in rat fibroblasts. *J Cell Sci* 109:2005–12.
45. Perera RM, et al. (2015) Transcriptional control of autophagy-lysosome function drives pancreatic cancer metabolism. *Nature* 524:361–365.
46. Harms E, Kern H, Schneider JA (1980) Human lysosomes can be purified from diploid skin fibroblasts by free-flow electrophoresis. *Proc Natl Acad Sci USA* 77:6139–6143.
47. Della Valle MC, et al. (2011) Classification of subcellular location by comparative proteomic analysis of native and density-shifted lysosomes. *Mol Cell Proteomics* 10:M110.006403.